Published in final edited form as:
FEBS Lett. 2008 August 20; 582(19): 2887–2892. doi:10.1016/j.febslet.2008.07.024.

Double-membrane gap junction internalization requires the clathrin-mediated endocytic machinery

Anna M. Gumpert, **Joseph S. Varco**, **Susan M. Baker**, **Michelle Piehl**, and **Matthias M. Falk***
Department of Biological Sciences, Lehigh University, 111 Research Drive, Iacocca Hall, Bethlehem, PA 18015, USA

Abstract

Direct cell-cell communication mediated by plasma membrane-spanning gap junction (GJ) channels is vital to all aspects of cellular life. Obviously, GJ intercellular communication (GJIC) requires precise regulation, and it is known that controlled biosynthesis and degradation, and channel opening and closing (gating) are exploited. We discovered that cells internalize GJs in response to various stimuli. Here we report that GJ internalization is a clathrin-mediated endocytic process that utilizes the vesicle-coat protein clathrin, the adaptor proteins AP-2 and Dab2, and the GTPase dynamin. To our knowledge, we are first to report that the endocytic clathrin machinery can internalize double-membrane vesicles into cells.

Keywords

Annular Gap Junctions; Clathrin; Connexins; Endocytosis; Gap Junctions; RNAi

1. Introduction

The role of clathin in vesicle endocytosis is well documented. Clathrin forms a typical curved lattice around endocytic vesicles that are internalized at the plasma membrane (PM) [1]. However, clathrin has also been implicated in the internalization of viruses, pathogenic bacteria, and even latex beads [2–4]. We have discovered an additional clathrin-mediated endocytosis (CME) process that results in the internalization of double-membrane vesicles from the PMs of cells that are coupled by gap junctions (GJs) [5].

GJs consist of transmembrane channels that bridge the PMs to provide direct intercellular communication. GJ channels cluster into so-called “plaques” containing a few to tens of thousands of channels. The channels facilitate diffusion of ions and small molecules, thus coupling the connected cells electrically and metabolically. GJ function has been determined vital for embryonic development, regulating differentiation and growth, and in maintaining tissue homeostasis. The essential role of GJ intercellular communication (GJIC) is manifested by numerous known mutations in GJ proteins, which have been linked to deafness, neuropathies, cataracts, skin disorders, and defects in cranio-facial development.

***Corresponding author:** Matthias M. Falk, PhD, Department of Biological Sciences, Lehigh University, 111 Research Drive, Iacocca Hall, D-218, Bethlehem, PA 18015, USA, Phone: 610-758-5896, Fax: 610-758-4004, Email: MFalk@lehigh.edu.

Two half-channels, or connexons, each synthesized by one of the coupled cells, dock head-to-head in the extracellular space to form the complete GJ channel. Six transmembrane proteins, termed connexins, oligomerize around a central hydrophilic pore to shape the connexon. Connexin proteins represent a large gene-family with connexin 43 (Cx43) being most ubiquitously expressed. It is evident, that GJIC needs to be regulated precisely for proper cellular function. GJ channel activity is regulated by both, channel opening and closing (gating) in response to physiological parameters, such as intracellular pH, Ca^{2+} concentration, and Cx phosphorylation [6–8], and by controlled channel biosynthesis and internalization [9,10]. Regulated GJ channel internalization, for example, is vital to cell migration and wound healing, as well as for cell division, when cells uncouple at beginning of mitosis, and re-couple at cytokinesis [11]; and misregulation of GJ channel internalization potentially leads to severe pathological conditions, such as cancer metastasis, pulmonary edema, ischemia, and hemorrhagic fevers.

We discovered that cells internalize their GJs in response to various endogenous and exogenous stimuli, including exposure to inflammatory mediators and nongenomic carcinogens [5] (Gilleron et al., manuscript submitted; Baker et al., manuscript in preparation). GJ internalization results in the formation of cytoplasmic double-membrane GJ vesicles (earlier termed annular GJs [AGJs]) that are degraded by lysosomal pathways. Interestingly, the GJ vesicle lumen and the inner vesicle membrane are derived from cytoplasm and PM of the neighboring cell, while the outer vesicle membrane is derived from the PM of the internalizing cell [5,12]. We further found that clathrin, and clathrin-associated proteins colocalize with internalizing GJs and GJ vesicles, suggesting a role for these proteins in GJ internalization [5]. Knocking down protein expression levels using RNA interference (RNAi), we now show that cellular depletion or functional inhibition of clathrin, the clathrin-adaptor proteins AP-2 and Dab2, and of the GTPase dynamin significantly inhibits GJ internalization.

2. Materials and Methods

2.1. Cell culture and connexin constructs

HeLa cells (CCL 2, American Type Culture Collection, Manassas, VA) were cultured under standard conditions as described [13]. For all experiments cells were grown on round 22 mm diameter glass cover slips coated with poly-L-lysine (Sigma-Aldrich, St. Louis, MO).

Cx43-GFP is described [13]. Cx43-mApple was constructed by replacing GFP by mApple cDNA [Shaner et al., in press].

2.2. RNAi knockdown (KD) procedures

All RNAi oligonucleotides (oligos) were purchased from Dharmacon RNA Technologies (Lafayette, CO). Clathrin heavy chain (CHC) oligos were SMARTpool option CLTC (M-004001-00). AP-2 α-Adaptin subunit RNAi oligos were SMARTpool option AP2 A1 (M-012492-00). Dab2 RNAi oligos were sequence 5'–UUCUUUAAGAGAAAAUCCAUU–3' published in [14]. Dynamin2 RNAi oligos were SMART pool option DNM2 (L–004007-00).

Previously described KD procedures were followed [5]. Briefly, oligonucleotides were transfected into HeLa cells using Oligofectamine (Invitrogen, Carlsbad, CA), followed 48 hours later by Cx43-GFP cDNA [13] using Superfect (Qiagen, Valencia, CA) as recommended by the manufacturers. Oligo transfection efficiency was tested using a fluorescent-labeled control (siGLO RISC-Free fluorescently-labeled, non-targeting oligonucleotide, Dharmacon) and was more than 90% efficient. Cells were assayed 72 hours after oligo transfection. Endocytosis inhibition was monitored by incubation in medium containing 10 μg/ml Alexa-

Fluor 488-labeled transferrin (5 mg stock solution in 1× PBS; Molecular Probes) for 3 minutes, fixation, and microscopic examination.

2.3. Immunoblot analyses

Verification of protein knockdown was assessed by Western blotting 72 hrs post RNAi transfection. Cells were scraped into PBS/protease inhibitor cocktail (Sigma-Aldrich). Cells were lysed in standard 5× sample buffer and boiled for 5 min. Samples were resolved on 10% Bis/Acrylamide (1:29) gels and transferred onto nitrocellulose membrane (pore size 0.2μm, Millipore Corporation, Bedford, MA). Following blocking, membranes were incubated in primary antibodies (1:1000 in 4% BSA in PBST) for 1hr at RT or o/n at 4°C. Membranes were washed in PBST for 15 min and incubated with horseradish peroxidase (HRP) - conjugated anti-mouse and anti-rabbit secondary antibody (1:5000 in 4% BSA in PBST, Zymed Laboratories) for 1hr at RT or o/n at 4°C. Immunoreactive bands were detected using an Immun-star HRP chemiluminescent kit (BioRad Laboratories, Hercules, CA). The signal was quantified by scanning developed films using SCION software (NIH).

2.4. Antibodies and immunofluorescence analyses

Mouse mAB anti-clathrin heavy chain (HCH) X22, a rabbit polyclonal antiserum directed against the β-subunit of AP-2 (GD/1, anti β1/β2), mouse mAB anti-α–Adaptin (AP-2 α-subunit) (MA1-64; Affinity BioReagents, Golden, CO), mouse mAB anti-α-Adaptin (610501; BD Biosciences, San Jose, CA), mouse mAB anti-Dab2 (p96, BD Biosciences), and mouse mAB anti-Dynamin2 (clone 41; BD Biosciences) were used at dilutions of 1:50-1:250 in 10% FBS/PBS. Secondary antibodies and immunofluorescence analyses have been described previously [5]. KD of proteins was evaluated by comparing the fluorescence intensity signals measured along lines on images taken under identical exposure conditions from treated and untreated cells.

2.5. Dynamin assays

Cells were transfected with Cx43-GFP, and 14 hours later dynamin function was inhibited by treating cells with 10 μM GTPγS (Sigma, 10 mM stock in water, for 5 hours), or with 40 μM dynasore 14 hrs post transfection and again with 20 μM dynasore 17hrs post transfection (Tocris Bioscience, Ellisville, MO, 20 mM stock in DMSO, for a total of 5 hrs). Additionally, cells were cotransfected with Cx43-mApple, and GFP-tagged dominant negative Dynamin2-K44A mutant. Number and size of GJs and GJ vesicles (AGJs) was evaluated 19 hours after transfections as described for the KD assays.

2.6. Statistical analyses

AGJs and GJs were counted on images taken of KD, drug treated and control cells in at least 3 independent experiments each. Only clearly defined GJs (a line of fluorescent puncta, or elongated plaques located between cell pairs), and AGJs (bright fluorescent spherical structures located in the cytoplasm ≥0.5 μm in diameter, see ref. [5]) were considered. Statistical analyses were performed using Microsoft Excel's analysis of variance (ANOVA) "Single Factor and Descriptive Statistics" functions of the data analysis package. For statistical analyses, the total number of AGJ vesicles was divided by the number of cell pairs that were positive for Cx43-GFP/-mApple expression and clearly coupled by GJs. Similarly, the total number and length of GJ plaques was determined and divided by the number of cell pairs. In all analyses, a p-value ≤0.05 was considered statistically significant.

3. Results

3.1. Depletion of clathrin significantly reduces GJ internalization

Using live-cell imaging, our lab and others have shown previously that cells internalize entire GJ plaques and plaque portions in a highly regulated process, with one cell of a pair preferentially budding GJs outward, and the other cell preferentially internalizing the double-membrane spanning GJ plaques [5,12]. We further found that internalizing GJs specifically colocalized with clathrin, the alternative clathrin adaptor Dab2, dynamin2, myosin-VI, and actin filaments, using both, monoclonal and polyclonal antibodies. Additionally, we found that cultivating Cx43-GFP transfected HeLa cells in hypertonic medium, a treatment described to prevent clathrin and adapter proteins from interacting [15], or depleting cells of clathrin using CHC RNAi significantly reduced GJ internalization by 56 and 55%, respectively [5]. Together, these investigations suggested a critical role for clathrin in the internalization of Cx43-based GJs. However, since clathrin is a major component of cellular metabolism, depletion of this protein could have reduced unspecifically Cx biosynthesis and trafficking, and thus GJ formation. If clathrin mediates the internalization of GJs, then clathrin depletion should correlate with a reduction of AGJ vesicles and a concomitant increase in GJ plaque size and/or number. To test this, we repeated RNAi-mediated CHC KD experiments in HeLa cells. Significant CHC depletion (>90%) at 72 hours post- RNA-oligo transfection was confirmed by Western blot analyses (Fig. 1A). In addition, immunofluorescence and fluorescence intensity analyses revealed significantly reduced CHC staining (Fig. 1B, C), and functional studies showed an almost complete inhibition of transferrin (Trfn) uptake (Fig. 1D, E), indicating efficient CHC depletion and CME inhibition.

CHC-depleted or control treated HeLa cells were transiently transfected with Cx43-GFP cDNA 48 hours post-RNAi transfection. In HeLa cells (that do not express endogenous Cxs), GJ plaques form only between transfected groups of cells (Fig. 2A, arrows). Cells were allowed to make and internalize GJ plaques for an additional 24 hours before fixation. Fields with clearly defined GJ plaques between cells were imaged (Fig. 2A, arrows), and AGJ and GJ plaque number and size were quantified (see Materials and Methods, Figure 2B–C). As in our previous study [5], we observed a significant reduction in the number of GJ vesicles that were internalized under CHC KD conditions (50% compared to control cells; Fig. 2B, C). In addition, we found a significant increase in the size and number of PM GJs (97% and 30% increase compared to control cells, Fig. 2B, C). Together, a decrease in internalized GJ vesicles, and a concomitant increase in GJ plaque size and number strongly suggests that GJ internalization is a clathrin-mediated process.

3.2. Depletion of clathrin adaptors significantly reduces GJ internalization

CME requires adaptor proteins that bind to both cargo and cargo receptors, and to clathrin to form endocytic vesicles. The adaptor protein complex AP-2 is commonly used for cargo internalization at the PM. Surprisingly, we detected only a very limited colocalization of AP-2 with internalizing GJs, or GJ vesicles [5]. On the other hand, we discovered a robust colocalization of the alternative clathrin adaptor protein Dab-2 with GJs and GJ vesicles, even in cells in which only low amounts of Dab2 are expressed [5]. Because of the prominent role of AP-2 in CME, and the pronounced colocalization of Dab2 with GJs/GJ vesicles, we examined whether either of these adaptors plays a critical role in GJ internalization. Thus, we performed RNAi-mediated KDs of these adaptor proteins in Cx43-GFP transfected HeLa cells. Efficient AP-2 and Dab-2 depletion was confirmed by Western blot analyses (>90%; Fig. 1A). A clear reduction of vesicular fluorescence signals (Fig. 1B, C), and significant inhibition of Trfn uptake was detected in the AP-2 depleted cells (Trfn uptake is known not to be affected in Dab2 depleted cells) [16] (Fig. 1D, E). Counting GJs and GJ vesicles in KD and control cells revealed that significantly fewer (38% and 28%) GJ vesicles were generated in the AP-2

and Dab2 KD cells, respectively (Fig. 2), while at the same time, GJ size and/or number increased significantly by 81% and 37% in AP-2, and 48% in Dab2 depleted cells (a slight, insignificant reduction in GJ number by 4% was observed in Dab2 depleted cells). Taken together, as observed for clathrin KD cells, depletion of either AP-2 or Dab-2 resulted in a statistically significant inhibition of GJ internalization, coinciding with an increase in GJ plaque size and/or number. These results strongly support a role for both adaptors in GJ internalization.

3.3. Depletion of dynamin significantly reduces GJ internalization

Another protein that is recruited to clathrin-coated pits is the GTPase dynamin, which functions in the completion of vesicle budding [17]. Since we also observed a robust colocalization of this protein with internalizing GJs and GJ vesicles [5], we depleted dynamin in Cx43-GFP expressing HeLa cells. Efficient dynamin2 (Dyn2) (the isoform expressed in HeLa cells) depletion was confirmed by Western blot analyses (>90%; Fig. 3A), and by a significant reduction of the vesicular dynamin2 fluorescence signal (Fig. 3B, C). Counting GJs and GJ vesicles in KD and control cells revealed that significantly fewer (29%) GJ vesicles were generated in the dynamin2 KD cells, while at the same time, GJ size increased significantly by 39% (Fig. 3F–H). Again, a slight insignificant reduction in GJ number by 9% was observed in these experiments.

Since the dynamin KD resulted in a less significant inhibition of GJ internalization than the clathrin KD (28% versus 50–55%), we decided to further investigate the role of dynamin in GJ internalization. We therefore overexpressed GFP-tagged dominant negative dynamin2-K44A mutant in Cx43-mApple expressing cells, or treated Cx43-GFP expressing HeLa cells either with the dynamin inhibitor, dynasore, or the GTPase inhibitor, GTPγS. All these treatments significantly inhibited transferrin uptake (Fig. 3D, E).

Counting GJs and GJ vesicles in drug-treated and control cells revealed that significantly fewer GJ vesicles were generated under these conditions (53, 50, and 33%, respectively Fig. 3G, H), while at the same time, GJ number and size increased significantly by 69 and 13% in Dyn2-K44A overexpressing cells. A reduction in GJ number and size by 11 and 25% was observed in dynasore treated cells and by 3 and 18% in GTPγS-treated cells, probably due to the general inhibition of GTPases by these drugs. Together, these results suggest that dynamin2 is also involved in GJ internalization.

Since all described protein depletions resulted in a reduced GJ internalization, and an increased GJ plaque size and/or number, we transfected cells with unrelated RNAi oligonucleotides (lamin A/C, expressed in HeLa cells; dynamin1, not expressed in HeLa cells; and a non-targeting oligo (siGLO RISC-Free). None of these control RNAi transfections had a significant impact on GJ internalization (data not shown).

4. Discussion

Using RNAi technology we down-regulated the expression of endocytic proteins and investigated the impact on GJ internalization. Proteins examined were found previously to co-localize with internalizing GJs [5]. We found a significant reduction of internalized GJs, and a concomitant significant increase in GJ size and/or number in all relevant KD experiments, indicating that GJ internalization is a clathrin-mediated process that also utilizes the clathrin adaptors AP-2 and Dab2, and the GTPase dynamin. A complete inhibition of GJ internalization was not observed in these KD experiments, possibly because (I) residual protein levels remained in the KD cells (<10%), (II) Cx43-GFP transfection and initial expression occurred at a time when KD protein levels were still significantly higher (48 versus 72 h), and/or (III)

cells may internalize GJs by an alternate clathrin-independent pathway, especially under conditions when CME is inhibited.

Although KD of AP-2 resulted in a significant reduction in GJ internalization (38%), we were unable to detect a convincing colocalization of this protein complex with internalizing GJs, (despite using antibodies directed either against the α- or the β- subunit) [5]. This might indicate that the relevant AP-2 epitopes are masked during its interaction with Cxs, or that AP-2 is only transiently, or to a limited extent involved in clathrin recruitment. The latter hypothesis is supported by our observation that AP-2 KD resulted in a less significant reduction in GJ internalization as compared to clathrin KDs (38% versus 50–55%), and by the fact that a second clathrin adaptor, Dab2, is recruited efficiently to internalizing GJs [5], and its depletion also resulted in significant reduction of GJ internalization (by 28%). Another possibility is that these clathrin adaptors act in concert, and/or that another, redundant clathrin adaptor is recruited in our KD experiments. Indeed, recent evidence suggests that numerous clathrin adaptors are localized within a single clathrin-coated vesicle [14], and that these adaptors have multiple, partially overlapping functions. Dab2, for example, can interact directly with cargo through a tyrosine-based internalization motif, with clathrin heavy chain, with the membrane lipid phosphatidylinositol-4,5-bisphosphate (PIP_2), and, through its C-terminal serine- and proline rich region, with myosin-VI to facilitate vesicle translocation [5,18]. Recently, a critical role for PIP_2 in CME has been shown [19]; and in $Dab2^{-/-}$ mice, LDL-receptor uptake (a typical Dab2 cargo), was found to be accomplished by the redundant clathrin adaptor ARH [20]. Interestingly, overlapping putative AP-2 and Dab2 internalization motifs are present in the C-terminus of Cx43 and of other connexins [5], and mutations within this region significantly increased the half-life of Cx43 [21].

We also found a pronounced colocalization of dynamin with GJs and internalized GJ vesicles [5]. Dynamin has been shown to be involved in the majority of endocytic processes [4,17,22, 23]. It is known to be recruited to clathrin-coated pits, and to contribute to the fission of clathrin-coated vesicles [17,24]. We found a significant, 29% less efficient internalization of GJs in dynamin KD cells, and experiments in which we inhibited dynamin function (GTPγS and dynasore treatment, or overexpression of GFP-tagged dominant negative Dyn2-K44A) reduced internalization by 33–53%, further supporting the role of dynamin in GJ internalization. Future research will address how, mechanistically, these proteins internalize double-membrane regions that can be 50 times larger than a typical endocytic vesicle [17].

Abbreviations used in this manuscript

AGJ, annular gap junction
AP-2, adaptor protein complex 2
CHC, clathrin heavy chain
CME, clathrin-mediated endocytosis
Cx, connexin
Dab2, disabled 2
GJ, gap junction
KD, knockdown
PM, plasma membrane
RNAi, RNA interference
Trfn, transferrin

Acknowledgements

We thank Linton Traub (University of Pittsburgh, PA, USA), Mark McNiven (Mayo Clinic, Rochester, MN, USA), Ramiro Massol and Tom Kirchhausen (Harvard Medical School, Boston, MA, USA), and Nathan Shaner and Roger Tsien (University of California San Diego, La Jolla, CA, USA) for kindly providing AP-2 antibodies, Dyn2 and

mApple cDNAs, and advise. This work was supported by NIHs NIGMS (grant GM55725), and the Bioengineering and Bioscience 2020 Funds.

References

1. Fotin A, Cheng Y, Sliz P, Grigorieff N, Harrison SC, Kirchhausen T, Walz T. Molecular model for a complete clathrin lattice from electron cryomicroscopy. Nature 2004;432:573–579. [PubMed: 15502812]
2. Aggeler J, Werb Z. Initial events during phagocytosis by macrophages viewed from outside and inside the cell: membrane-particle interactions and clathrin. J. Cell Biol 1982;94:613–623. [PubMed: 6813339]
3. Rust MJ, Lakadamyali M, Zhang F, Zhuang X. Assembly of endocytic machinery around individual influenza viruses during viral entry. Nat. Struct. Mol. Biol 2004;11:567–573. [PubMed: 15122347]
4. Veiga E, Cossart P. Listeria hijacks the clathrin-dependent endocytic machinery to invade mammalian cells. Nat. Cell Biol 2005;7:894–900. [PubMed: 16113677]
5. Piehl M, Lehmann C, Gumpert A, Denizot JP, Segretain D, Falk MM. Internalization of large double-membrane intercellular vesicles by a clathrin-dependent endocytic process. Mol. Biol. Cell 2007;18:337–347. [PubMed: 17108328]
6. Delmar M, Coombs W, Sorgen P, Duffy HS, Taffet SM. Structural bases for the chemical regulation of Connexin43 channels. Cardiovasc. Res 2004;62:268–275. [PubMed: 15094347]
7. Moreno AP. Connexin phosphorylation as a regulatory event linked to channel gating. Biochim. Biophys. Acta 2005;1711:164–171. [PubMed: 15955301]
8. Solan JL, Marquez-Rosado L, Sorgen PL, Thornton PJ, Gafken PR, Lampe PD. Phosphorylation at S365 is a gatekeeper event that changes the structure of Cx43 and prevents down-regulation by PKC. J. Cell Biol 2007;179:1301–1309. [PubMed: 18086922]
9. Berthoud VM, Minogue PJ, Laing JG, Beyer EC. Pathways for degradation of connexins and gap junctions. Cardiovasc. Res 2004;62:256–267. [PubMed: 15094346]
10. Musil LS, Le AC, VanSlyke JK, Roberts LM. Regulation of connexin degradation as a mechanism to increase gap junction assembly and function. J. Biol. Chem 2000;275:25207–25215. [PubMed: 10940315]
11. Stein LS, Boonstra J, Burghardt RC. Reduced cell-cell communication between mitotic and nonmitotic coupled cells. Exp. Cell Res 1992;198:1–7. [PubMed: 1727042]
12. Jordan K, Chodock R, Hand AR, Laird DW. The origin of annular junctions: a mechanism of gap junction internalization. J. Cell Sci 2001;114:763–773. [PubMed: 11171382]
13. Falk MM. Connexin-specific distribution within gap junctions revealed in living cells. J. Cell Sci 2000;113:4109–4120. [PubMed: 11058097]
14. Keyel PA, Mishra SK, Roth R, Heuser JE, Watkins SC, Traub LM. A single common portal for clathrin-mediated endocytosis of distinct cargo governed by cargo-selective adaptors. Mol. Biol. Cell 2006;17:4300–4317. [PubMed: 16870701]
15. Heuser JE, Anderson RG. Hypertonic media inhibit receptor-mediated endocytosis by blocking clathrin-coated pit formation. J. Cell Biol 1989;108:389–400. [PubMed: 2563728]
16. Mishra SK, Keyel PA, Hawryluk MJ, Agostinelli NR, Watkins SC, Traub LM. Disabled-2 exhibits the properties of a cargo-selective endocytic clathrin adaptor. EMBO J 2002;21:4915–4926. [PubMed: 12234931]
17. Conner SD, Schmid SL. Regulated portals of entry into the cell. Nature 2003;422:37–44. [PubMed: 12621426]
18. Brett TJ, Traub LM. Molecular structures of coat and coat-associated proteins: function follows formc. Curr. Opin. Cell Biol 2006;18:395–406. [PubMed: 16806884]
19. Zoncu R, Perera RM, Sebastian R, Nakatsu F, Chen H, Balla T, Ayala G, Toomre D, De Camilli PV. Loss of endocytic clathrin-coated pits upon acute depletion of phosphatidylinositol 4,5-bisphosphate. Proc. Natl. Acad. Sci., U S A 2007;104:3793–3798. [PubMed: 17360432]
20. Maurer ME, Cooper JA. The adaptor protein Dab2 sorts LDL receptors into coated pits independently of AP-2 and ARH. J. Cell Sci 2006;119:4235–4246. [PubMed: 16984970]

21. Thomas MA, Zosso N, Scerri I, Demaurex N, Chanson M, Staub O. A tyrosine-based sorting signal is involved in connexin43 stability and gap junction turnover. J. Cell Sci 2003;116:2213–2222. [PubMed: 12730291]

22. Gold ES, Underhill DM, Morrissette NS, Guo J, McNiven MA, Aderem A. Dynamin 2 is required for phagocytosis in macrophages. J. Exp. Med 1999;190:1849–1856. [PubMed: 10601359]

23. Pelkmans L, Pèuntener D, Helenius A. Local actin polymerization and dynamin recruitment in SV40-induced internalization of caveolae. Science 2002;296:535–539. [PubMed: 11964480]

24. Bonifacino JS, Glick BS. The mechanisms of vesicle budding and fusion. Cell 2004;116:153–166. [PubMed: 14744428]

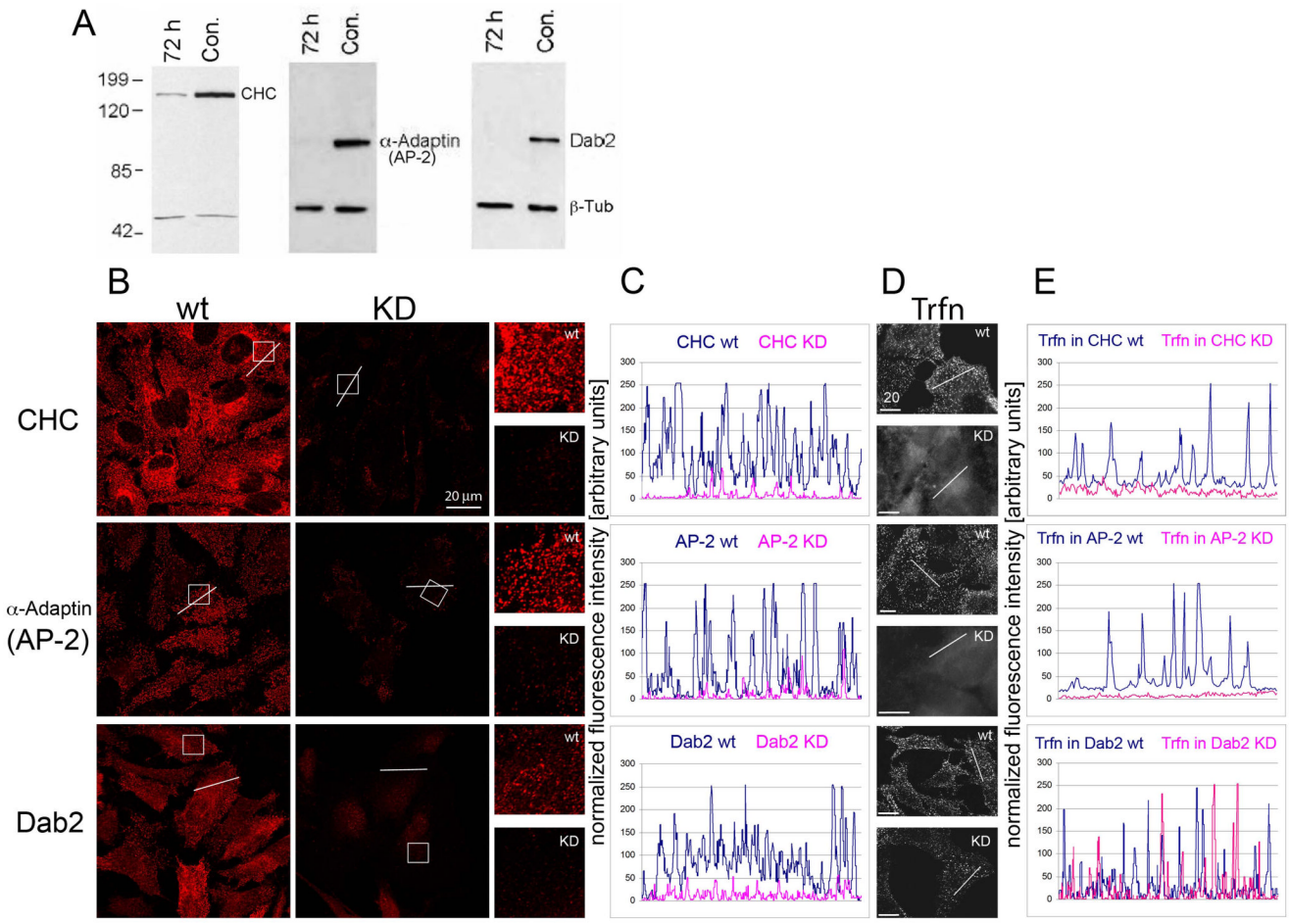

Fig. 1. RNAi-mediated KD of clathrin heavy chain (CHC), and the clathrin adaptors α-Adaptin (AP-2) and Dab2 in HeLa cells

(A) Over 90% of respective protein levels were depleted when assayed 72 h post oligo transfection by Western blot analyses. Equal gel loading was verified by β-tubulin (β-Tub) staining. **(B)** Efficient protein depletion verified by immunofluorescence staining (images were captured at identical parameters). Boxed areas are shown enlarged on the right. **(C)** Blots of fluorescence intensity measured along respective lines (shown in the images in B). **(D)** Inhibition of CME monitored by fluorescence labeled transferrin (Trfn) uptake. **(E)** Blots of fluorescence Trfn intensity measured along respective lines (shown in the images in D).

A

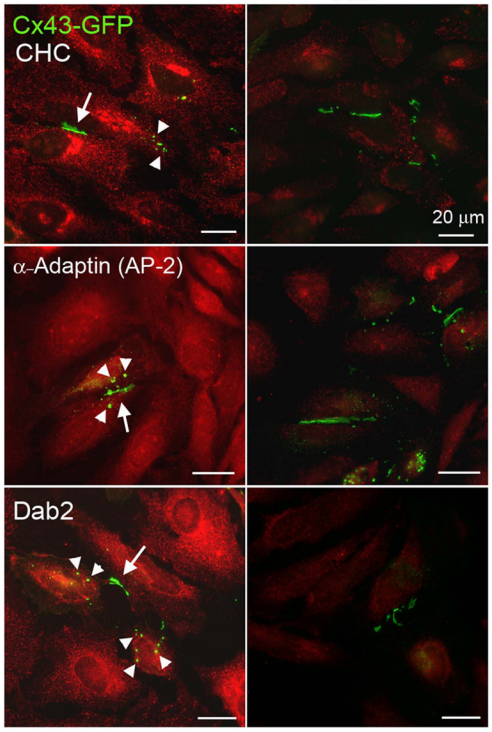

B

	CHC			α-Adaptin (AP-2)			Dab2		
	mock	KD	%	mock	KD	%	mock	KD	%
Ave # of AGJs per cell pair	16.0	8.0	-50	14.6	9.1	-38	14.8	10.6	-28
Ave # of GJ plaques per cell pair	2.7	3.5	30	2.6	4.7	81	2.6	2.5	-4
Ave GJ length per cell pair [μm]	15.3	30.1	97	15.0	20.6	37	15.5	23.0	48
Total # of cell pairs	129	121		76	68		73	71	
Total # of AGJs	2064	972		1112	621		1079	752	
Total # of GJ plaques	350	426		196	318		193	175	
Total GJ plaque length [μm]	1980	3640		1139	1401		1131	1631	

C

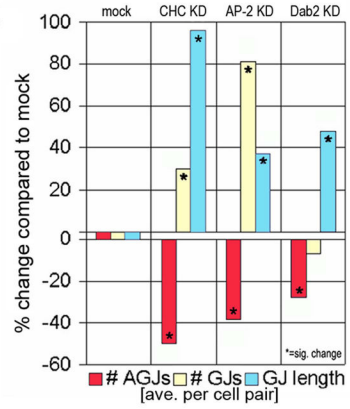

Fig. 2. GJ internalization is significantly reduced in CHC, α-Adaptin and Dab2 RNAi-treated cells

(A) Representative images of mock (wt), and RNAi- (KD) treated cells with Cx43-GFP GJs (arrows), and internalized GJ vesicles (arrowheads) marked. **(B, C)** Quantitative analyses of total and average GJ length (blue) and numbers (yellow), and numbers of internalized GJs (red) per cell pair in KD and control cells.

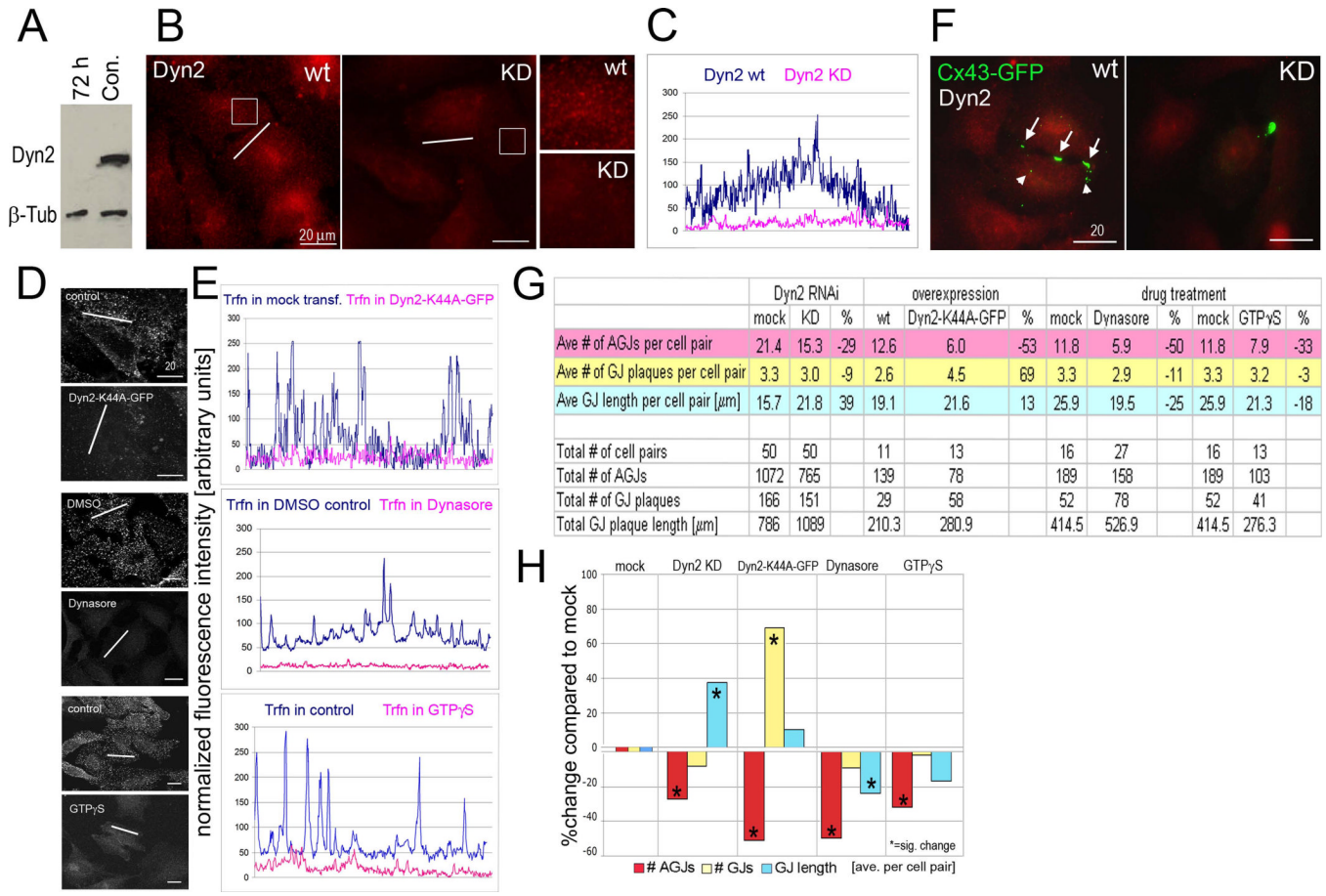

	Dyn2 RNAi			overexpression			drug treatment					
	mock	KD	%	wt	Dyn2-K44A-GFP	%	mock	Dynasore	%	mock	GTPγS	%
Ave # of AGJs per cell pair	21.4	15.3	-29	12.6	6.0	-53	11.8	5.9	-50	11.8	7.9	-33
Ave # of GJ plaques per cell pair	3.3	3.0	-9	2.6	4.5	69	3.3	2.9	-11	3.3	3.2	-3
Ave GJ length per cell pair [μm]	15.7	21.8	39	19.1	21.6	13	25.9	19.5	-25	25.9	21.3	-18
Total # of cell pairs	50	50		11	13		16	27		16	13	
Total # of AGJs	1072	765		139	78		189	158		189	103	
Total # of GJ plaques	166	151		29	58		52	78		52	41	
Total GJ plaque length [μm]	786	1089		210.3	280.9		414.5	526.9		414.5	276.3	

Fig. 3. RNAi-mediated depletion and functional inhibition of dynamin significantly reduces GJ internalization

(A) Efficient Dyn2 protein depletion verified by Western blot analysis, and **(B)** immunofluorescence staining (images were captured at identical parameters). Boxed areas are shown enlarged on the right. **(C)** Plots of fluorescence intensity measured along respective lines (shown in the images in B). **(D)** Inhibition of CME in HeLa cells overexpressing dominant negative Dyn2-K44A-GFP mutant, or were treated with Dynasore, or GTPγS monitored by fluorescence labeled Trfn uptake. **(E)** Plots of fluorescence Trfn intensity measured along respective lines (shown in the images in D). **(F)** Representative images of mock (wt), and Dyn2 RNAi- (KD) treated cells with Cx43-GFP GJs (arrows), and internalized GJ vesicles (arrowheads) marked. **(G, H)** Quantitative analyses of total and average GJ length and numbers, and numbers of internalized GJs per cell pair in treated and control cells.